Journal of Zhejiang University-SCIENCE A in press
www.jzus.zju.edu.cn; www.springer.com/journal/11582
E-mail: jzus_a@zju.edu.cn

Research Article
https://doi.org/10.1631/jzus.A2500641

Morphodynamics and controlling mechanisms of subaqueous crescentic dunes in the western offshore region of Hainan Island

Hang SUN[1,2,3], Qi ZHANG[2], Botao XIE[2], Bo MIAO[4,5], Lizhong WANG[1]✉, Guoxin LI[6], Yufei LI[7], Qin GAO[8]

[1]*Ocean College, Zhejiang University, Zhoushan 316021, China*
[2]*Engineering Research and Design Institute, CNOOC Research Institute, Beijing 100028, China*
[3]*Zhejiang Key Laboratory of Offshore Civil Engineering and Materials, Zhejiang University, Hangzhou 310058, China*
[4]*Institute of Coastal Systems - Analysis and Modeling, Helmholtz-Zentrum Hereon, Geesthacht 21502, Germany*
[5]*Institute of Oceanography, Center for Earth System Research and Sustainability, University of Hamburg, Hamburg 20148, Germany*
[6]*CNOOC China Ltd., Tianjin Branch, Tianjin 300450, China*
[7]*China Oilfield Services Limited (COSL), Tianjin 300459, China*
[8]*Advanced Nantong Institute of Southeast University, Nantong 226010, China*

Abstract: Subaqueous dunes hold significant research value in sedimentary geomorphology and marine engineering. Based on two phases of multibeam bathymetric surveys conducted in the western offshore region of Hainan Island, this study systematically examines the geometric characteristics and dynamic evolutionary mechanisms of subaqueous dunes. The results show that dune formation is governed by multiple interacting factors, including hydrodynamics, sediment transport processes, and water depth, with tidal currents serving as the primary driving force for dune initiation and growth. Dune evolution is jointly modulated by the interplay between bedload transport and suspended sediment concentration. The lag effect of suspended sediments represents a key mechanism contributing to dune development, while dune morphological stability is constrained by suspended sediments as well as by limitations imposed by water depth. Specifically, crest erosion suppresses further increases in dune height, whereas water depth regulates the critical scale of dune growth. Subaqueous crescentic dune height plays a dominant role in controlling morphological stability and hydrodynamic response, whereas dune width exhibits strong linear relationships with both height and wavelength, highlighting its integrative role in linking vertical and horizontal morphological development. The growth of crescentic dunes proceeds through four successive stages: initiation, chasing, merging, and splitting. Throughout this evolutionary sequence, sediment supply plays a crucial role in regulating dune wavelength and shaping the overall morphology. Correspondingly, dune geomorphology evolves sequentially from crescentic to curved, bifurcated, and ultimately linear forms. This study offers theoretical support and practical insights for understanding seabed geomorphic evolution, regional sediment dynamics, and marine engineering applications.

Key words: Subaqueous dunes; Tidal current dynamics; Suspended sediment; Growth scale; Water depth control; Dynamic evolution

1 Introduction

Crescentic dunes are asymmetric bedforms that typically develop under unidirectional flow conditions and limited sediment supply. Named for their characteristic crescentic morphology, these dunes are widely distributed across terrestrial arid zones, riverbeds, subaqueous environments, and the surfaces of Mars and other terrestrial planets (Bagnold, 1941; Howard et al., 1978; Greeley and Iversen, 1985; Ashley, 1990; Lancaster, 1995; Flemming, 2000; Bourke et al., 2008). Their formation is governed by a combination of hydrodynamic forces, sediment availability, surface moisture, and bed characteristics (Fryberger and Dean, 1979; Hugenholtz and Wolfe, 2005).

A typical crescentic dune consists of three fundamental components: the stoss (upstream) slope, the lee (slip face) slope, and two downcurrent horns that extend in the direction of transport (Sauermann et

✉ Lizhong WANG, wanglz@zju.edu.cn

Received Dec. 7, 2025; Revision accepted Apr. 9, 2026; Crosschecked

al., 2000; Andreotti et al., 2002; Hersen, 2004). Sediment particles are transported along the stoss slope to the dune crest and deposited on the slip face due to flow deceleration and boundary layer separation. Recirculation zones at the horns capture part of the sediment, while the remainder is released downstream, maintaining mass balance and enabling steady dune migration (Bagnold, 1941). Studies have shown that crescentic dunes exhibit consistent attractor behavior, in which their morphology tends to converge toward a stable and recurring configuration across a wide range of spatial and temporal scales, from centimeter-scale laboratory flumes over minutes to kilometer-scale aeolian environments over millennia (Claudin and Andreotti, 2006).

In recent years, advances in experimental, computational, and remote sensing techniques have significantly expanded our understanding of dune formation and evolution. These include subaqueous flume experiments (Assis and Franklin, 2020), wind tunnel experiments (Liang et al., 2025), satellite image analysis (Rubanenko et al., 2022), numerical simulations (Zhang et al., 2024), and machine learning–based morphometric classification (Rubanenko, 2024). Experimental findings indicate that processes such as dune coalescence, horn calving, and collision exhibit high sensitivity to initial spacing, dune scale, and flow velocity, showing strong nonlinear responses (Ewing and Kocurek, 2010;). Sediment grain-size distribution has been identified as a key factor influencing dune morphology, including height, wavelength, and symmetry (Liang et al., 2025). Additionally, the concept of inertial length, which describes the lag distance required for a particle to reach the flow velocity, has been recognized as a fundamental control on dune self-organization (Hersen et al., 2002). Beyond steady-state flows, increasing attention has been directed toward unsteady hydrodynamic disturbances in natural settings. In the northern South China Sea, internal waves, especially internal tides and internal solitary waves, can generate near-bed currents exceeding 80 cm/s and thereby substantially modify seabed sediment transport processes (Ma et al., 2016). These internal waves exert contrasting influences on dune migration: obliquely incident internal solitary waves tend to drive upslope movement, while periodic internal tides promote downslope migration, revealing complex, event-driven sediment dynamics.

Despite significant progress in both theoretical understanding and methodological approaches, several key limitations remain in the current research on crescentic dune formation and evolution. First, most experimental studies rely heavily on the assumption of local similarity under idealized laboratory conditions, which fails to capture the complexity of nonlinear interactions among multiple environmental factors in natural systems. Second, remote sensing and laboratory observations have predominantly focused on terrestrial aeolian dunes or small-scale flume-generated bedforms, resulting in a severe lack of systematic investigations into large-scale or deep-water subaqueous crescentic dunes. Third, due to limitations in current seabed observation technologies, high-resolution and repeatable long-term datasets remain extremely scarce, impeding our ability to fully decipher the formation processes, spatiotemporal variability, and dominant control mechanisms of these submarine landforms.

This study focuses on the nearshore region off the western coast of Hainan Island in the northwestern South China Sea, where subaqueous dunes are extensively developed. Two fundamental questions arise in this setting: What are the dominant factors controlling dune formation and evolution? Is there an upper limit to their morphological development? To address these questions, we analyze two sets of high-resolution multibeam bathymetric datasets to systematically quantify the geometric parameters of the dunes, including height-to-width ratios, wavelengths, and crest angles. These morphometric analyses are integrated with regional hydrodynamic data to identify the key mechanisms governing dune formation and migration. The primary objective of this research is to advance the mechanistic understanding of crescentic dune evolution in complex deep-water environments, thereby enriching the theoretical framework of planetary geomorphology and subaqueous sediment dynamics. In addition, the findings are expected to provide scientific guidance for marine engineering planning and contribute to risk assessments related to submarine geological hazards.

2 Study area

The study area is located in the nearshore region off the southwestern coast of Hainan Island on the northern continental shelf of the South China Sea. Geographically, it lies on the southeastern flank of the Beibu Gulf and extends approximately 25 km offshore, representing a typical depositional environment of a shallow continental shelf (Fig. 1). Water depths within the area range from 20 to 60 meters, covering a total surface area of approximately 60 km^2. The seabed topography is highly irregular, characterized by the widespread presence of sand bars, sand ridges, shallow troughs, and ripple-like bedforms, forming a hierarchically superimposed system of sedimentary microgeomorphic units. The coastline exhibits an overall north–south (N–S) orientation and stretches approximately 80 km in length. The coastal zone is dominated by Neogene coastal depositional landforms, and the regional stratigraphy consists primarily of Quaternary sand- and gravel-rich clay layers overlying granite bedrock (Xia et al., 2001).

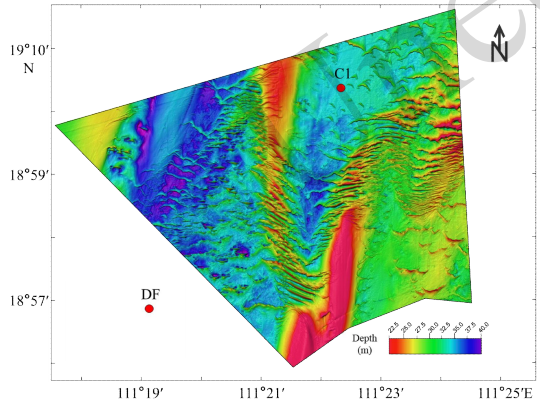

Fig. 1 Overview of the seafloor topography and dune distribution in the study area off western Hainan Island. C1 denotes the station for current velocity and suspended sediment measurements.

The study area is situated within a tropical monsoon climate zone characterized by high temperatures, abundant precipitation, and distinctly seasonal wind regimes. During summer, southeasterly winds prevail, while in winter, the dominant winds shift to the northeast. This periodic reversal of wind direction exerts a significant influence on regional wave structures and nearshore sediment transport dynamics (Ma et al., 2016). Based on in situ current measurements during the winter of 2021, tidal currents in the region exhibit a pronounced bidirectional pattern, predominantly flowing along *NW–SE* and *SW–NE* directions, forming a typical alongshore current system. Wave observations recorded at station DF from November 2021 to November 2022 show that the regional wave regime is dominated by mixed waves (59.7%), followed by wind waves (30.8%) and swell waves (9.5%). The maximum wave height (H_{max}) reached 7.44 m, while the maximum and mean significant wave heights (H_m) were 4.1 m and 0.94 m, respectively. The dominant spectral peak periods were concentrated between 4 and 6 seconds, with prevailing wave directions oriented toward the north (*N*) and south–southeast (*SSE*), reflecting the influence of southeasterly monsoon winds on the regional wave climate.

From a geomorphological perspective, the seabed in the study area features a diverse array of submarine dunes, prominently including crescentic dune systems. These bedforms are predominantly aligned along *N–S* or *NW–SE* axes and form part of a complex, multiscale self-organizing sedimentary system. Many of these dunes are associated with secondary ripples and smaller-scale dunes, and some barchan dunes exceed 10 meters in height, making them one of the most representative flow-controlled geomorphic units in the region. Notably, dune orientation exhibits marked spatial heterogeneity: dunes in the western sector tend to incline northward, while those in the eastern sector slope southward. This spatial asymmetry reflects the influence of directional tidal forcing and localized hydrodynamic disturbances on sediment deposition patterns.

3. Data and methods

3.1. Data acquisition and observation equipment

This study integrates hydrodynamic and geomorphological data collected through two sets of comprehensive field campaigns. Full-tide synchronous hydrological observations were conducted between December 2021 and January 2022 to capture the complete tidal cycle and assess hydrodynamic conditions under different tidal phases. High-resolution multibeam bathymetric surveys were carried out from October to December 2021 and again from November 2022 to January 2023, enabling full-area coverage of the seabed morphology.

High-resolution bathymetric data were obtained using the Kongsberg EM710 multibeam echosounder system, with a horizontal resolution of 5 m × 5 m and a depth accuracy better than ±5 cm. This resolution is sufficient to identify and characterize submarine bedforms ranging from centimeter-scale sand ripples to dunes with wavelengths of several hundred meters, including crescentic dunes. Postprocessing was performed using Fledermaus software to construct digital terrain models (DTMs) and extract dune morphology metrics. Hydrodynamic measurements were conducted at station C1, which is a flat and open area with crescentic dunes, using a combination of an acoustic Doppler current profiler (ADCP) and a point current meter. Routine measurements of current velocity and direction were taken at 1-hour intervals, with increased sampling frequency (every 30 minutes) during critical tidal phases such as maximum flood, maximum ebb, and slack water. All velocity data were processed using a 100-second moving average to minimize the influence of high-frequency noise. The point current meter was set to record continuously at 1-minute intervals. Vertically, six-layer profiling was implemented at depths corresponding to the surface (0.5 m below the water surface), 0.2D, 0.4D, 0.6D, 0.8D, and near-bottom (0.5 m above the seabed), where D denotes the local water depth, ensuring comprehensive coverage of the vertical current structure.

The suspended sediment concentration (SSC) measurements were carried out at the same stations as the current velocity observations using a point-integration method and standard horizontal suspended sediment samplers. During each sampling event, at least 1000 mL of water was collected, and all samples were thoroughly mixed prior to analysis to ensure homogeneous suspension. SSC sampling was synchronized with the current measurements and conducted at regular hourly intervals over complete tidal cycles during three representative tidal conditions: from 11:00 on 4 January to 12:00 on 5 January 2022 (spring tide), from 09:00 on 7 January to 10:00 on 8 January 2022 (mean tide), and from 12:00 on 12 January to 13:00 on 13 January 2022 (neap tide).

The temperature resolution was maintained at ≤0.05 °C with an accuracy of ±0.2 °C, while the salinity resolution was ≤0.05‰ with an accuracy of ±0.2‰. The salinity stratification coefficient, as defined by Prandle (1985), is expressed by the following equation:

$$N = \frac{S_d - S_b}{\overline{S}} \tag{1}$$

where S_d and S_b represent the salinity values at the bottom and surface layers, respectively, and $\overline{S}$ denotes the depth-averaged salinity.

3.2. Data processing and analytical methods

3.2.1. Geometric parameters and migration rate of crescentic dunes

This study classifies the different types of dunes in the research area based on their geomorphological characteristics, categorizing them into four types: crescentic dunes, curved dunes, bifurcated dunes, and linear dunes (Fig. 2a). Additionally, statistical analysis is conducted on the characteristic parameters and migration velocities of these four dune types. The geometric framework of crescentic dunes in the study area is illustrated in Fig. 2b. These bedforms migrate progressively in the direction of the dominant hydrodynamic forcing, typically aligned with the prevailing current. Key morphological parameters are defined as follows: L Mean wavelength of the dune body, measured crest-to-crest along the primary migration direction. L_1: Length from the stoss slope toe to the crest. L_2: Length from the crest to the lee slope toe. W: Dune width, measured perpendicular to the migration direction. H: Dune height, defined as the vertical relief between crest and trough. α : Angle of the lee slope (gentle slope). β : Angle of the stoss slope (steep slope). λ (symmetry index): A dimensionless parameter describing the asymmetry of the dune, defined as $\lambda = (L_1 - L_2)/L$ (Fig. 2c).

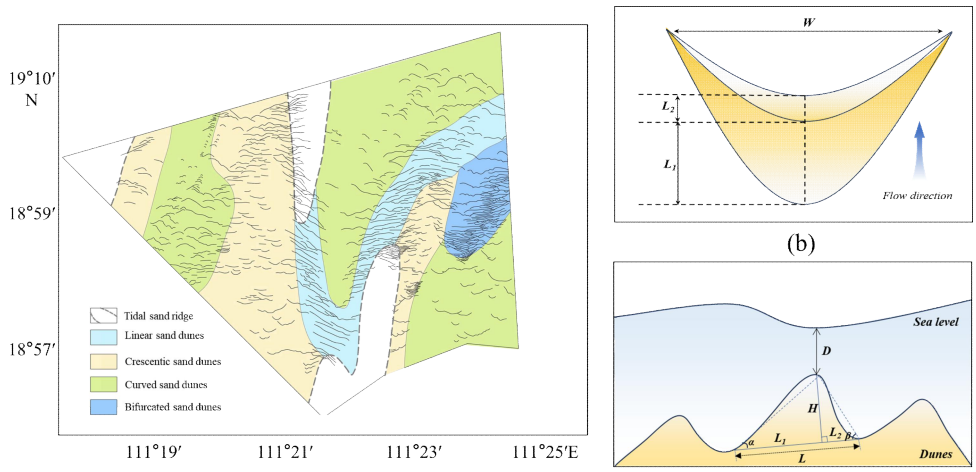

Fig. 2 Distribution of subaqueous dune types and statistical methods for parameter analysis: (a) distribution of dune types in the study area; (b) characteristic parameters of crescentic dunes; (c) statistical analysis of subaqueous dune parameters.

The migration distance was determined by applying the fast Fourier transform (FFT) method to extract phase information from corresponding morphological profiles of the two survey periods. Phase shifts between the two temporal datasets were then calculated to infer the downstream displacement of dune crests along the dominant flow direction. This approach effectively mitigates the influence of local asymmetrical variations in bedform geometry and enhances the robustness of intersurvey shape comparisons.

3.2.2. Analysis and calculation of dune morphological parameters

In this study, we adopt the formulations proposed by van Rijn (1984; 1993; 2007) to compute the ratio of sediment shear velocity to settling velocity (u_*/w_s), which serves as a diagnostic indicator for determining the dominant sediment transport mode at each observation station within the study area:

$$u_* = \sqrt{g}\frac{u}{\theta} \tag{2}$$

$$\theta = 18\log\left(\frac{12D}{k_s'}\right) \tag{3}$$

$$w_s = \frac{10\nu}{D_{50}}\left[\sqrt{1+\frac{0.01(s-1)gD_{50}^3}{\nu^2}}-1\right]^2 \tag{4}$$

$$s = \frac{\rho_s}{\rho_w} \tag{5}$$

where u_* is the shear velocity; u represents the depth-averaged flow velocity; θ is the Chezy roughness coefficient; k' is the sediment roughness, typically defined as $k' = 2.5D_{50}$; w_s is the particle settling velocity; ν is the kinematic viscosity, with $\nu = 1\times10^{-6}$ m^2/s; ρ_s is the sediment density, ρ_s = 2 650 kg/m^3; ρ_w is the density of seawater, ρ_w =1 025 kg/m^3.

To further quantify the transport intensity and directionality of sediment across the dune field, this study adopts the semiempirical formulation proposed by Bartholdy et al. (2002) to compute the unit-width sediment transport rate and the net flux during flood and ebb tides. The sediment transport formulation (Eq. 7) follows Bartholdy et al. (2002), which represents a simplified form of the classical total load transport model proposed by Engelund and Hansen (1967). The relevant expressions are provided in Equations (6)–(10).

$$q_{sb} = 0.5u_f^3u^2d^{-1} \tag{6}$$

$$u_f = \frac{u_z}{\left(8.5+2.5\ln\left(\frac{z}{k}\right)\right)} \tag{7}$$

$$k = \frac{d}{12} \tag{8}$$

$$V_D = \left(6+2.5\ln\left(\frac{D}{k}\right)\right)u_f \tag{9}$$

$$Q_{sb} = q_{sb}\times T \tag{10}$$

where q_{sb} is the unit sediment transport rate per unit width ($kg \cdot m^{-1} \cdot s^{-1}$); u_z is the velocity at measurement height z above the bed ($m \cdot s^{-1}$); u_f is the friction velocity ($m \cdot s^{-1}$); d is the median grain diameter (m); k is the bed roughness (m); z is the measurement height of the tidal current (m); Q_{sb} is the mean unit-width sediment flux ($kg \cdot m^{-1}$); T is the time (s).

Bartholdy (2015) proposed the virtual boundary layer theory, establishing a predictive model for dune height based on sediment grain size, flow velocity, and water depth (Eqs. 11–12). Although this model was originally developed for current ripples with characteristic heights on the order of 10 cm, its underlying mechanism provides valuable insight into dune-scale morphodynamics. According to the theory, dune height influences the friction velocity at the crest through boundary layer adjustment. When the bedform height is small, the virtual boundary layer remains thin, resulting in a relatively high crest friction velocity. As the dune grows, the boundary layer thickens, and the logarithmic velocity profile increasingly governs the flow structure, causing the rate of increase in crest friction velocity to diminish. Eventually, a critical state is reached where the friction velocity at the dune crest attains a minimum. This minimum represents a dynamically stable equilibrium condition in which further vertical growth is suppressed by enhanced crest erosion.

$$H_{\text{mean}} = 0.068L^{0.81} \tag{9}$$

$$H_{\max} = 0.160L^{0.84} \tag{10}$$

where H_{mean} is the mean dune height (m); $H_{\max}$ is the maximum dune height (m).

4. Results

4.1. Analysis of the environmental conditions for the formation of subaqueous crescentic dunes

The analysis of the water body conditions in the study area is a key factor in reversing the formation and evolution of dunes. The mixing intensity and stratification of the water body are important factors affecting the vertical diffusion capacity of suspended sediments, while the concentration of suspended sediments severely limits dune growth and constrains the increase in dune wave height (Van Landeghem et al., 2009). The calculated values of the salinity stratification coefficient revealed that it was –0.00015 during spring tide, –0.00012 during neap-spring transitional tide, and 0 during neap tide—all significantly below the threshold value of 0.01. Notably, the coefficients during the spring and transitional tides were negative, indicating a typical well-mixed water column at the observed station. Under these conditions, the density stratification effect induced by salinity is extremely weak, allowing suspended sediments to diffuse freely in the vertical direction. This further suggests that the water column maintains a strong capacity for vertical material exchange, facilitating sediment resuspension and transport throughout the tidal cycle.

The statistical analysis of vertical variations in suspended sediment concentration across observation stations indicates a clear stratified distribution pattern within the water column of the study area (Fig. 3). The average concentration of suspended sediment in the surface layer was measured at 17.7 mg/L, while the bottom layer exhibited a higher average value of 21.4 mg/L. Overall, the suspended sediment concentration increases progressively from the surface to the bottom, suggesting that sediment resuspension and bottom turbulence are more active near the seabed. During spring tide conditions, the suspended sediment concentration averaged 22.4–28.6 mg/L throughout the tidal cycle. For the mean tide, suspended sediment concentrations ranged from 20.0 to 25.5 mg/L, whereas during the neap tide they were much lower, averaging 9.7 to 10.2 mg/L. This pattern, with concentrations decreasing from spring tide to mean tide and then to neap tide, indicates that suspended sediment concentration increases markedly with tidal strength. These results suggest that tidal current intensity is a primary control on sediment resuspension and vertical distribution in the study area. The density stratification driven by salinity was negligible and had no significant effect on the vertical diffusion of suspended sediments.

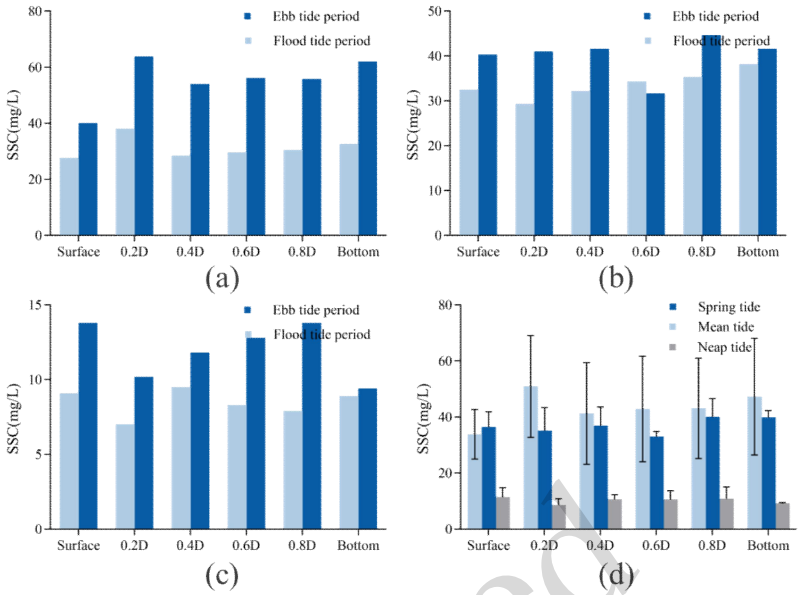

Fig. 3 Vertical distribution characteristics of suspended sediment concentration at Station C1: (a) spring tide; (b) mean tide; (c) neap tide; (d) comparison of suspended sediment concentrations under different tidal conditions

4.2. Morphological characteristics analysis of crescentic dunes

Based on field measurements from the study area, this section quantitatively investigates the interrelationships among key morphological and environmental parameters of crescentic dunes. A total of 29 crescentic dunes were measured and analyzed. The analysis revealed a strong positive correlation between H and both the steepness index and the mean lee slope angle, with correlation coefficients of 0.60 and 0.77, respectively. This suggests that dune height plays a dominant role in determining the morphological stability and hydrodynamic response of crescentic dunes (Fig. 4). In contrast, L exhibited a negative correlation with these two parameters (r = –0.68 and –0.32, respectively), indicating that wavelength has a comparatively weaker influence on morphological evolution. These findings are consistent with previous research (van Dijk P. M., 1999), which noted that during the steepening stage of dune growth, height tends to dominate over wavelength in controlling dune evolution.

Furthermore, a positive correlation was observed between L and λ, implying that longer dunes tend to exhibit greater symmetry and that wavelength exerts a regulatory influence on dune shape balance. Correlation plots also indicate a moderate positive relationship between V and D, with a coefficient of approximately 0.50, suggesting that water depth is a key environmental factor influencing dune mobility. The migration rate showed a weak negative correlation with H ($r \approx -0.37$) and no significant correlation with L ($|r| < 0.3$). Additionally, D was weakly negatively correlated with both H ($r \approx -0.30$) and λ ($r \approx -0.39$), suggesting that deeper water may impose geometric constraints on dune development.

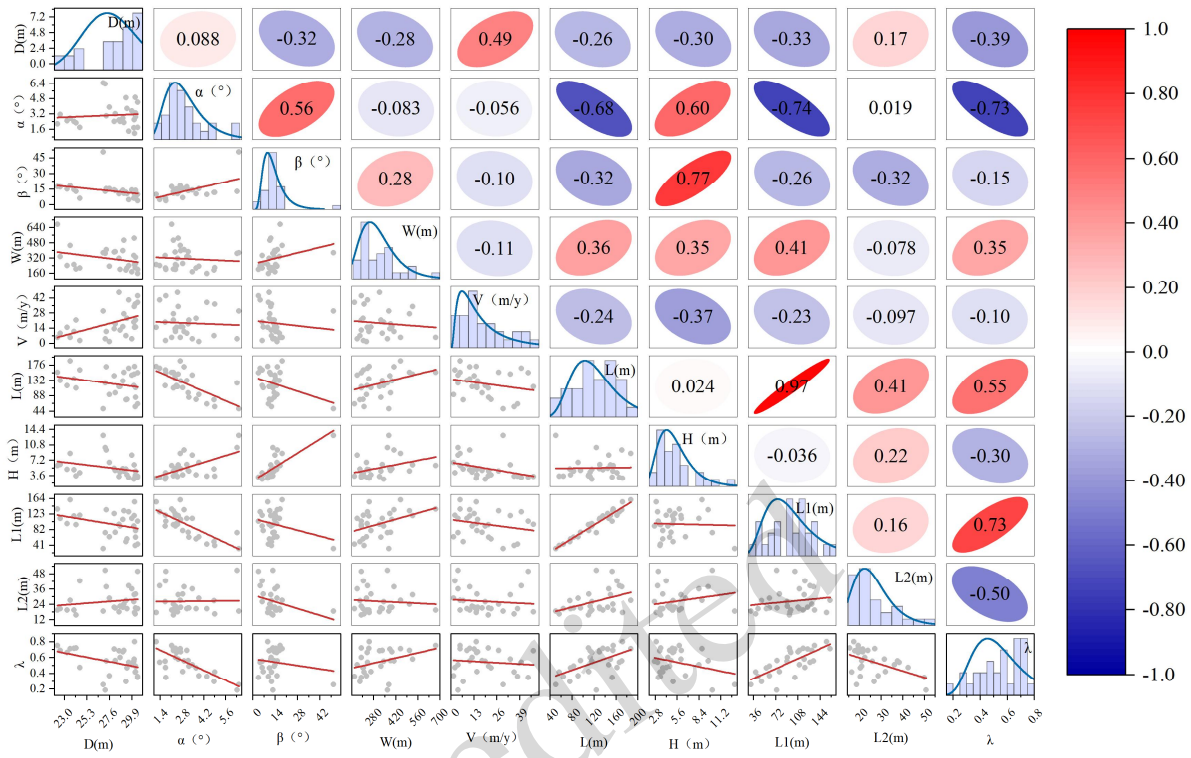

Fig. 4 Correlation analysis among the morphological parameters of crescentic dunes

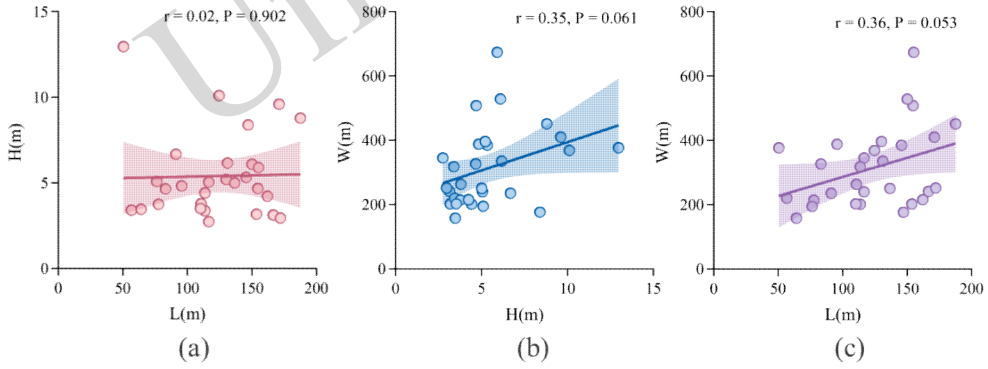

Fig. 5 Analysis of crescentic dune morphological parameters and migration velocity (a) Dune length vs. height; (b) Height vs. width; (c) Wavelength vs. width

Based on statistical analysis of 38 crescentic dunes within the study area, the dune wavelength ranges from 50 to 200 meters, while the dune height ranges primarily from 2 to 6 meters, with occasional maxima reaching up to 10 meters. In general, dune height exhibits a positive correlation with wavelength; however, the rate of increase in height significantly diminishes with increasing wavelength and, in some cases, even declines. A critical dune height threshold is observed at approximately 11 meters, corresponding to approximately 1/4 to 1/3 of the local water depth. The emergence of this height limit is likely controlled by the interplay between hydrodynamic forces and sediment transport capacity. These morphometric parameters offer valuable insights into the genesis of crescentic dunes in the study area. For most dunes, the height is less than 0.25 times the local water depth, indicating that they are primarily shaped under modern hydrodynamic conditions (Terwindt, 1971; Francken et al., 2004). Furthermore, statistical analysis of L, H, W, and λ indicates that dune width exhibits stronger and more

consistent correlations with other morphometric parameters than height or wavelength alone (Fig. 5). In contrast to the negligible relationship between dune height and $H = 0.04\ L$, $R = 0.02$), which suggests little direct coupling between vertical growth and longitudinal scale, dune width shows clear linear dependencies on both height and wavelength. These results highlight dune width as a key morphometric parameter that integrates vertical and horizontal development processes and plays a central role in defining the geometric structure of crescentic dunes.

5. Discussion

5.1. Analysis of controlling factors of crescentic dunes

5.1.1. Sedimentological conditions

Sediment transport characteristics constitute one of the key controlling factors in the formation and morphodynamic evolution of crescentic dunes. Quantitative evaluation of sediment transport modes under varying tidal conditions enables the assessment of whether a dune is undergoing accretion or erosion, which holds significance for both regional geomorphic evolution and coastal engineering design. Based on Equations (2)–(5), the ratio of shear velocity to particle settling velocity u_*/w at station C1 during spring tide is 0.113, while the values for neap and mean tides are 0.046 and 0.080, respectively. When $u_*/w_s<1$, the dominant sediment transport mode is bedload transport. This mode facilitates the growth and morphological development of dunes, thereby promoting increases in both dune height and wavelength.

Based on Equations (6)–(10), the unit-width sediment transport rate and the net sediment flux at station C1 during flood and ebb tides were quantitatively calculated. The results reveal that the net sediment transport direction in the study area predominantly trends southwestward, with the magnitude of transport gradually decreasing from spring tide to neap tide (Table 1). During spring tide, the transport flux reaches its maximum of 24.07 $kg \cdot m^{-1} \cdot d^{-1}$, highlighting the significant influence of hydrodynamic forcing on sediment transport intensity. The overall sediment transport pattern of the crescent-shaped dunes also exhibits a southwestward orientation, consistent with the net sediment transport direction. This alignment indicates that both hydrodynamic conditions and sediment transport jointly govern the migration behavior of crescentic dunes in the region.

Table 1 Sediment transport fluxes during flood and ebb tides under different tidal conditions in the study area

Tidal type	Flood tide sediment transport ($kg \cdot m^{-1} \cdot d^{-1}$)	Direction (°)	Ebb tide sediment transport ($kg \cdot m^{-1} \cdot d^{-1}$)	Direction (°)	Nep tide sediment transport ($kg \cdot m^{-1} \cdot d^{-1}$)
Spring tide	57.42	13	81.50	205	-24.07
Mean tide	19.92	4	1.38	202	+18.53
Neap tide	0.90	5	1.31	121	-0.41

5.1.2. Analysis of suspended sediment conditions under tidal currents

The suspended sediment concentration is a critical indicator reflecting the degree of seabed erosion and is directly influenced by tidal current dynamics, which in turn govern the growth and vertical development of crescentic dunes. In the study area, crescentic dunes are primarily shaped by tidal currents, with wave-induced sediment mobilization playing a relatively minor role (Sun et al., 2025). Under turbulent conditions, the suspended sediment concentration exhibits pronounced cyclic fluctuations in response to tidal phases, while vertical stratification remains weak. This observation highlights the dominant role of tidal currents in driving intratidal sediment transport, whereas waves mainly control seasonal variability (Chen, 2004; Cao, 1993). During a complete tidal cycle, the intensification of current velocity enhances erosion and scouring of surface sediments. Once the flow exceeds the critical threshold for sediment entrainment, particles are mobilized into suspension, leading to a sharp increase in the near-bed suspended sediment concentration. Subsequently, these sediments diffuse vertically under turbulent mixing, resulting in elevated concentrations in the mid- and upper water columns. As the current subsides, the flow weakens, resuspension diminishes, and

sedimentation occurs, leading to a decrease in suspended sediment concentration.

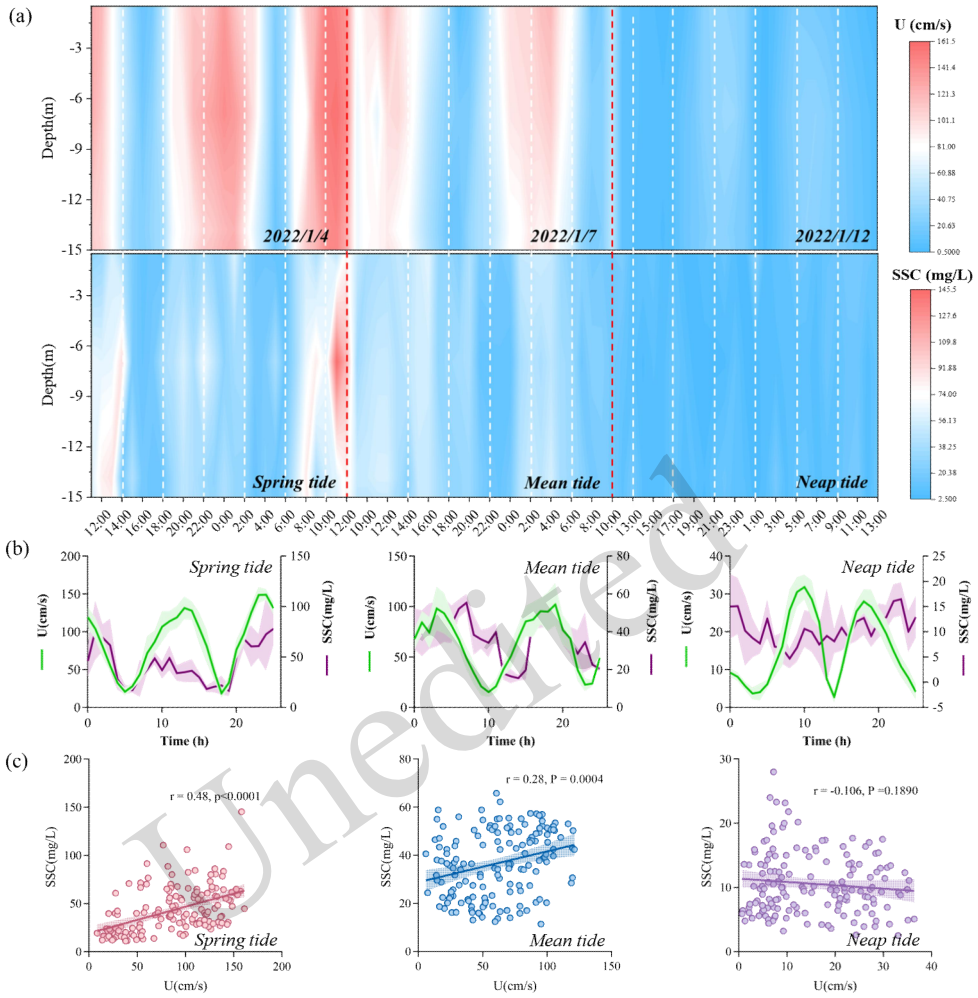

Fig. 6 (a) Time–depth profiles of tidal current velocity and suspended sediment concentration at Station C1; (b) Temporal variations in current velocity and suspended sediment concentration; (c) Linear relationship between current velocity and suspended sediment concentration

To characterize the temporal variability of sediment suspension, time-series profiles of current velocity and suspended sediment concentration were constructed for station C1 (Fig. 6). The analysis reveals a significant positive correlation between the suspended sediment concentration and tidal current velocity. During spring tides, strong hydrodynamic conditions promote pronounced seabed erosion and sediment resuspension, resulting in elevated suspended sediment concentrations. In contrast, during mean tides, sediment resuspension mainly occurs during the flood phase, whereas the ebb phase, characterized by flow velocities below the critical threshold, favors sediment settling. Additionally, due to the lag in sediment response to hydrodynamic forcing, suspended sediment concentrations often trail behind current velocity peaks, exhibiting a "lag effect" of approximately 1–2 hours. Over the course of a full tidal cycle, suspended sediment concentrations exhibit complex variability, typically presenting 2–3 peaks during the observation period at each station. During neap tides, both flood and ebb currents remain below the critical entrainment threshold, leading to a dominance of sediment deposition and a marked reduction in suspended sediment concentrations. In summary, spring tides, characterized by intensified hydrodynamic mixing and weak water-column stratification, promote the vertical diffusion of suspended sediments and thereby facilitate dune growth. In contrast, neap tides are

associated with relatively weak hydrodynamic conditions, stronger stratification, and limited sediment transport capacity, which favor sediment deposition and the morphological stabilization of crescentic dunes.

5.1.3. Analysis of water depth as a controlling factor

Water depth is one of the key environmental factors governing the formation and evolution of crescentic dunes. Flemming (2000) pointed out that in shallow-water environments, dune height and wavelength are often closely correlated with water depth, whereas this correlation tends to weaken in deeper settings. Crescentic dunes tend to develop in areas with relatively coarse sediments, strong current velocities, and limited sediment supply, conditions that favor stable bedform development and morphological evolution. As dunes grow vertically, the flow velocity over the crest increases due to topographic amplification; if this velocity becomes excessive, it may inhibit further vertical accretion. Additionally, when suspended sediment transport dominates, the dune crest becomes more susceptible to erosion, potentially resulting in a decrease in wave height (Van Landeghem et al., 2009). Observational studies by Terwindt (1971) and Francken et al. (2004) revealed that dune height rarely exceeds one-quarter of the local water depth, thereby providing an empirical upper limit for dune growth.

In the present study area, the water depth ranges from 12 to 57 meters, with crescentic dunes primarily distributed within the 20–32 m depth range. The shallower zone (<22 m) is located within the central part of the N–S trending giant sand ridge field, where dune development is limited due to narrow ridge spacing, minimal relief, and reduced flow velocities at the ridge crests. In contrast, no dunes were observed in the deeper zone (>50 m), where bottom currents are likely insufficient to initiate sediment motion. The most active dune field is found within the 20–32 m depth interval, where hydrodynamic conditions are dominated by tidal currents. In this zone, dune wavelengths range from 0 to 200 m, and heights range from 1 to 14 m, indicating that water depth, in conjunction with seabed topography and current strength, defines a suitable morphological window for dune formation. These findings suggest that water depth can modulate dune wavelength, height, and migration rate by influencing bottom current velocity, sediment transport mode, and topographic constraints.

Bagnold (1941) previously proposed that in aeolian environments, the minimum stable dune height is approximately 1 meter, with lengths no shorter than 10 meters, implying the existence of a lower physical threshold for dune formation. Experimental work by Hersen (2002) further indicated an inverse relationship between dune migration rate and height, offering theoretical support for dynamical models despite scale limitations. Morphometric analyses of large-scale subaqueous dunes by Ashley (1990) and Flemming (1988, 2000) similarly indicate empirical scaling relationships between dune height and wavelength, as well as upper limits linked to water depth. In the present study, statistical analysis of 38 measured crescentic dunes yields an average height of approximately 5.8 m, with maximum values reaching 14.0 m. The observed critical dune height approaches approximately one-quarter of the local water depth, consistent with previously reported empirical constraints. Application of the virtual boundary layer framework under current-dominated conditions predicts average and maximum dune heights of 5.3 m and 14.1 m at a water depth of 30 m, corresponding to relative differences of 9.8% and 2.2%, respectively. Rather than demonstrating strict predictive equivalence, this agreement suggests that water depth exerts a fundamental control on the critical dune height through hydrodynamic regulation. It should be noted that the study area is characterized by mixed wave–tide forcing; however, near-bed hydrodynamic observations indicate that dune-forming phases are predominantly governed by tidal currents. Therefore, the model application is restricted to current-dominated intervals. As emphasized by Allen (1968) and Yalin (1972), although dune height is strongly correlated with water depth, dune geometry is also influenced by sediment grain size, current velocity, and sediment supply, which collectively modulate morphodynamic evolution.

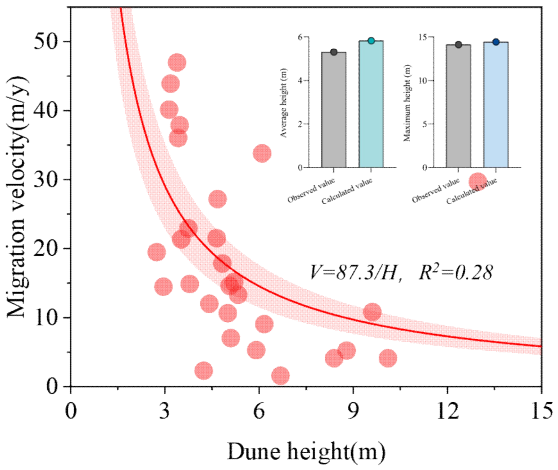

Fig. 7 Relationship between crescentic dune height and migration velocity

5.2. Migration and evolution of crescentic dunes

The dynamic development of subaqueous crescentic dunes proceeds through several stages (Fig. 8). Initially, sediment grains are mobilized under the influence of prevailing currents and shear stress, forming incipient crescentic dunes at the 0.01–0.1 m scale. These nascent dunes are characterized by relatively low heights and fast migration speeds, governed by localized sediment supply and hydrodynamic conditions (Fig. 8a). During this phase, both dune height and wavelength gradually increase, representing the early-stage morphological evolution. Subsequently, dunes enter an overtaking and coalescence phase. Due to their small volume and higher mobility, newly formed crescentic dunes can catch up and merge with larger upstream dune bodies. When dune dimensions exceed the saturation length of the sediment transport system, the sediment flux Q becomes nearly independent of dune height H, leading to an inverse relationship between migration velocity V and height H (Bagnold, 1941). This results in increased dune size but decreased migration speed as overall mass accumulates (Hersen, 2002). Moreover, interdune spacing imposes a constraint on individual growth (Flemming, 1988). When spacing is narrow, backflow disturbances from downstream dunes reinforce upstream dune accretion, inhibiting further migration and eventually inducing coalescence and dynamic equilibrium. Field observations reveal that small dunes commonly "merge" with larger upstream dunes after overtaking. Conversely, when large dunes approach smaller downstream dunes, the local flow field is altered. Enhanced return flow and increased flow resistance upstream limit sediment supply to the downstream dune, making it more susceptible to being "consumed" and absorbed by the larger dune (Fig. 8b). For instance, in the northeastern section of the study area, ebb currents dominate over weaker flood currents. The upstream flood current restricts the development of downstream dunes, while ebb flow, shielded by larger dunes, further promotes coalescence by capturing smaller dune bodies (Fig. 8c).

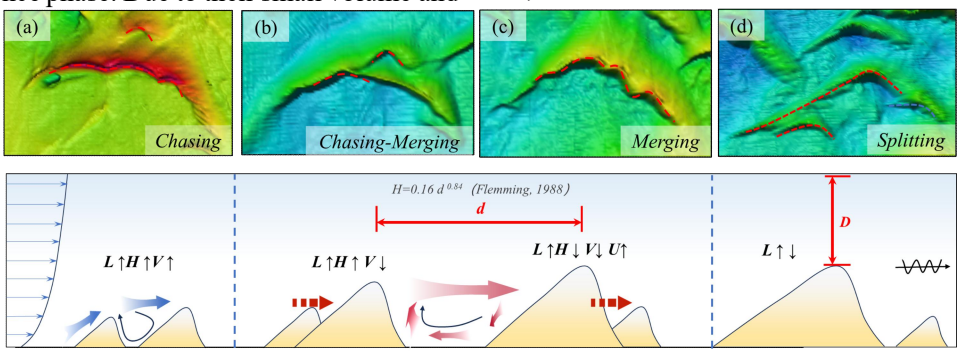

Fig. 8 Schematic diagram of the dynamic growth and evolution process of subaqueous crescentic dunes. (a) Chasing; (b) Chasing-Merging; (c) Merging; (d) Splitting; Arrows (↑/↓) indicate the increase or decrease in dune morphological parameters during evolution. d represents the spacing between adjacent dunes.

Finally, the crescentic dunes enter the crossing and separation stage (Fig. 8d). As discussed in Section 5.1.3, dune growth is constrained by environmental thresholds. When the dune height gradually approaches its theoretical maximum, hydrodynamic erosion at the dune crest induces a state of morphological stability, and a further height increase is suppressed. During the preceding overtaking and merging phase, the dune wavelength continues to grow while the dune height approaches its critical

limit, leading the dune system toward a dynamic equilibrium state. However, under conditions of continuous sediment supply, smaller dunes with relatively high migration velocities may still crossover saturated, larger dune bodies. Schwämmle and Herrmann (2005) proposed that this "crossing" behavior represents a mass exchange process rather than true geometric traversal. The sediment composition of the rear dune differs from that of the leading dune, suggesting the formation of a new unit rather than the persistence of an original dune body. Prior to reaching the saturation state, merging is the dominant evolutionary pathway. Once the dune height nears its theoretical maximum, crossing and separation become more frequent. During this stage, dune morphology is shaped by the dual influences of hydrodynamic disturbance and continuous sediment supply, reflecting a pattern of relative morphological stability interrupted by localized restructuring. With persistent sediment input, dune wavelengths further elongate, slopes become gentler, and sediment spreads laterally along the main current direction.

As the crescentic dune system progressively approaches a state of dynamic equilibrium under environmental constraints, dune height stabilizes, migration velocity decreases, and wavelength continues to increase (Fig. 9). Under conditions of sustained and large-scale sediment supply, the overall evolutionary framework of crescentic dunes gives rise to new morphological types. With continued growth and development, dunes undergo collision and coalescence under tidal forcing, gradually evolving into curved dunes (Fig. 9b). Following collision and merging, both the wavelength and amplitude increase further, and the migration direction aligns with the dominant current.

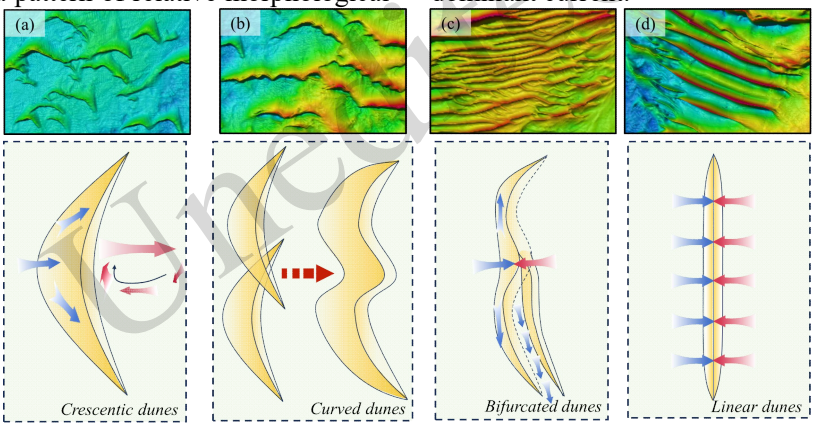

Fig. 9 Four stages in the growth and evolution of subaqueous dunes: (a) crescentic dunes; (b) curved dunes; (c) bifurcated dunes; (d) linear dunes

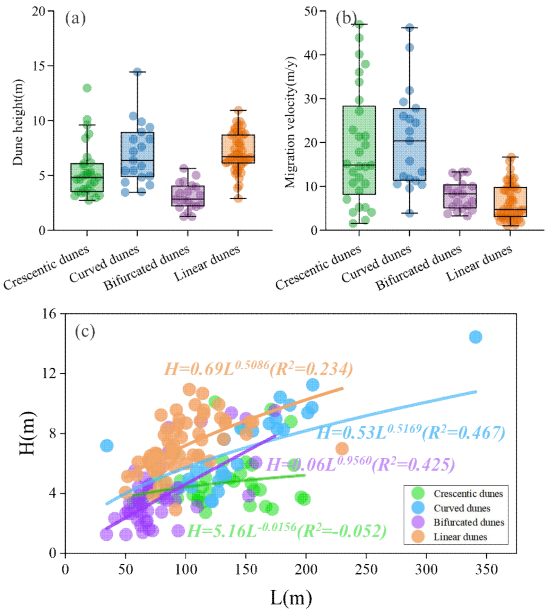

Fig. 10 Morphometric characteristics of different types of subaqueous dunes: (a) distribution of dune heights; (b) distribution of dune migration rates; (c) fitted relationship between dune wavelength and height

As the sediment supply continues, the distance between the curved dunes shortens. With ongoing dune evolution, a dense dune field forms, and the migration speed of the dunes slows down (Fig. 10a and 10b). At this point, bifurcation phenomena start to emerge within the curved dunes, gradually evolving into secondary bifurcated dunes. As a result, the wavelength and amplitude of the bifurcated dunes further decrease (Figs. 9c and 10c). The bifurcated dunes typically originate from the "footslope" of the curved dunes. Due to uneven tidal dynamics, sediment converges at convex slope angles. As the wave amplitude increases, tidal currents disperse at the concave sides of the crescentic dunes, and sediment accumulates at convex angles. Under hydrodynamic conditions, semienclosed or closed bifurcated dunes are gradually formed. These bifurcated dunes exhibit typical dual-peak or unidirectional sediment transport. The tidal currents on both the incoming and outgoing phases are similar, and the bottom currents transport sediment along the dune slopes. The spaces between dunes serve as sediment transport channels, where sediment accumulates, giving rise to secondary sand waves on the surfaces of both primary and secondary dunes. This results in the formation of overlapping, interwoven bifurcated dunes of varying sizes. Due to the hydrodynamic compression and transport of water along the channel sides, the space in the channel may be closed or semiclosed, thus presenting unidirectional sediment transport. The secondary sand waves at the ends of these channels often exhibit high symmetry. The orientation of secondary sand waves in semienclosed channels indicates that sediment transport between bifurcated dune channels is predominantly unidirectional.

Linear dunes, on the other hand, are relatively stable, reflecting a more balanced and stable tidal hydrodynamic environment (Fig. 9d). The wave heights typically do not exceed 10 meters, and wavelengths range from 50 to 200 meters. Under similar tidal conditions, fully open channels form between the dunes, with bidirectional sediment transport occurring between these channels, leading to the formation of linear sand waves (Zhou et al., 2019). Over prolonged tidal influences, continuous sediment accumulation and replenishment cause the wavelength of the sand waves to increase again, and the increase in wave height is particularly noticeable. No secondary sand waves form between linear dunes. In the open space, tidal currents transport sediment along the crest of the dunes, and sediment cannot accumulate between the dune bottoms, further increasing the wave height.

Research indicates that the migration and evolution of subaqueous crescentic dunes in the study area follow a typical "chase-merge-overcome-rebalance" evolutionary chain. Initially, individual dunes grow rapidly and merge forward, and then the wave heights stabilize under environmental constraints. Some dunes experience "overcoming" or reseparation under dynamic disturbances, and the system as a whole enters a dynamic equilibrium phase. With the continuous supply of sediment, the crescentic dunes evolve under hydrodynamic forces, forming curved dunes, bifurcated dunes, and linear dunes in the dune morphology sequence.

5.3. Limitations and future prospects for subaqueous crescentic dunes

This study builds upon a comprehensive review of previous research on dune formation and evolution, integrating field measurements of suspended

sediment transport, water depth, and dune geometric parameters from the western offshore region of Hainan Island. It reveals the formation and evolutionary processes of large-scale subaqueous crescentic dunes within the 30–60 m water depth range under tidally dominated environments, as well as the upper growth limits of dunes. These findings provide empirical support for understanding the critical scale and stability mechanisms governing dune development. Furthermore, the evolutionary model of subaqueous crescentic dunes established in this study can be extended to analogous dune systems on terrestrial planets, offering new perspectives and a reference framework for interpreting the formation and evolution of aeolian dunes (e.g., Martian dunes). This highlights the interdisciplinary scientific significance and potential engineering applications of the study. Despite these advances, several limitations remain. Due to constraints in observational data resolution and the lack of time-series quantification, the formation mechanisms of centimeter-scale small sand waves still require further validation through physical experiments. In particular, the initial formation processes of sand waves under varying sediment supply conditions and microscale hydrodynamic forcing remain insufficiently understood. In addition, the critical thresholds governing the morphological transitions of crescentic dunes, their growth limits, and the controlling parameters have not yet been quantitatively constrained.

Future research will focus on the formation and evolution mechanisms of small-scale sand waves. Physical model experiments will be conducted to further investigate the quantitative relationships among sediment supply, hydrodynamic conditions, and morphological evolution. Meanwhile, by integrating findings from aeolian sand waves and Martian dune studies, efforts will be made to develop a cross-scale, dimensionally consistent model for sand wave–dune evolution, aiming to reveal the universal principles governing dune system evolution under different environmental conditions.

6. Conclusions

Based on two sets of multibeam bathymetric survey data collected from the western offshore area of Hainan Island, this study systematically analyzed the geometric characteristics and dynamic evolution mechanisms of subaqueous dunes. The main conclusions are as follows:

The formation and evolution of dunes are subject to multiple controls, including hydrodynamic forces, sediment transport properties, and water depth. Dune formation is primarily controlled by tidal currents, and bedload transport during spring tides is the key mechanism driving sustained dune growth. The dune evolution process is jointly modulated by sediment transport and suspended sediment concentration. The lag effect of suspended sediments is identified as a critical mechanism, wherein the processes of deposition and resuspension exert a significant regulatory influence on dune growth. The stabilization of dune morphology results from the combined constraints of crest erosion and water depth, with crest erosion limiting the increase in dune height and water depth regulating the spatial scale of dune development.

Correlation analysis of dune geometric parameters indicates that dune height plays a dominant role in determining the morphological stability and hydrodynamic response of subaqueous crescentic dunes. Dune width exhibits clear linear dependencies on both height and wavelength and thus represents a key morphological parameter that integrates vertical growth and horizontal development processes.

The growth of crescentic dunes involves four successive stages: initiation, chasing, merging, and splitting. Correspondingly, their morphology evolves from crescentic to curved, bifurcated, and eventually linear forms. Water depth plays a crucial role in regulating the critical height of dunes by modulating tidal flow conditions. Meanwhile, sediment supply significantly affects dune wavelength and morphology, acting as a key driver for the dynamic evolution of the dune system.

Acknowledgments

This work is supported by the Key Technologies and Engineering Demonstration for Flow Safety and Geological Hazard Evaluation in the Development of Ultra-Deep Water and Ultra-Shallow Gas Fields (KJ202500282), the Key Program of the National Natural Science Foundation of China, Dynamic Catastrophic Mechanism and Design Theory of

Typhoon-Induced Offshore Wind Power Structures (No. 52238008), and a subproject of the National Key Science and Technology Major Project, Mechanisms and Analytical Techniques for Soil–Pile Interaction in Deepwater Complex Foundations (No. 2024ZD1403304-4).

Author contributions

Hang SUN designed the research. Qi ZHANG and Botao XIE processed the corresponding data. Hang SUN wrote the first draft of the manuscript. Bo MIAO, Lizhong WANG, Guoxin LI, Yufei LI, and Qin GAO helped to organize the manuscript. Lizhong WANG and Qin GAO revised and edited the final version.

Conflict of interest

Hang SUN, Qi ZHANG, Botao XIE, Bo MIAO, Lizhong WANG, Guoxin LI, Yufei LI, and Qin GAO declare that they have no conflict of interest.

Data availability

The data that support the findings of this study are available from the corresponding author upon reasonable request.

References

Allen JRL, 1968. The nature and origin of bed-form hierarchies. *Sedimentology* 10(3): 161–182. https://doi.org/10.1111/j.1365-3091.1968.tb01110.x

Andreotti B, Claudin P, Douady S, 2002. Selection of dune shapes and velocities Part 1: Dynamics of sand, wind and barchans. *European Physical Journal B* 28: 321–339. https://doi.org/10.1140/epjb/e2002-00236-4

Assis WR, Franklin EM, 2020. A comprehensive picture for binary interactions of subaqueous barchans. *Geophysical Research Letters* 47(18): e2020GL089464. https://doi.org/10.1029/2020GL089464

Ashley M, 1990. Classification of large-scale subaqueous bedforms; a new look at an old problem. *Journal of Sedimentary Research* 60(1): 160–172. https://doi.org/10.2110/jsr.60.160

Bagnold RA, 1941. The physics of blown sand and desert dunes. Methuen, London.

Bartholdy J, Bartholomä A, Flemming BW, 2002. Grain-size control of large compound flow-transverse bedforms in a tidal inlet of the Danish Wadden Sea. *Marine Geology* 192(1–3): 27–44. https://doi.org/10.1016/S0025-3227(02)00419-X

Bartholdy J, Ernstsen VB, Flemming BW, Winter C, Bartholomä A, Kroon A, 2015. On the formation of current ripples. *Scientific Reports* 5: 11390. https://doi.org/10.1038/srep11390

Bourke MC, Edgett KS, Cantor BA, 2008. Recent aeolian dune change on Mars. *Geomorphology* 94(1–2): 247–255. https://doi.org/10.1016/j.geomorph.2007.05.012

Engelund F, Hansen E, 1967. A monograph on sediment transport in alluvial streams. Technical report, Technical University of Denmark, Copenhagen. https://resolver.tudelft.nl/uuid:81101b08-04b5-4082-9121-861949c336c9

Cao ZD, Wang GF, 1993. Numerical simulation of wave lifting sand and tidal current transporting sand. *Acta Oceanologica Sinica* 15(1): 107–118. (in Chinese)

Chen SL, Zhang GA, Yang SL, et al., 2004. Temporal and spatial changes of suspended sediment concentration and resuspension in the Yangtze River Estuary and its adjacent waters. *Acta Geographica Sinica* 59(2): 260–266. (in Chinese)

Claudin P, Andreotti B, 2006. A scaling law for aeolian dunes on Mars, Venus, Earth, and for subaqueous ripples. *Earth and Planetary Science Letters* 252(1): 30–44. https://doi.org/10.1016/j.epsl.2006.09.004

Ewing RC, Kocurek G, 2010. Aeolian dune-field pattern boundary conditions. *Geomorphology* 114(3): 175–187. https://doi.org/10.1016/j.geomorph.2009.06.015

Flemming BW, 1988. Zur Klassifikation subaquatischer, strömungstransversaler Transportkörper. Bochumer Geologische und Geotechnische Arbeiten 29: 44–47.

Flemming BW, 2000. The role of grain size, water depth and flow velocity as scaling factors controlling the size of subaqueous dunes. In Marine Sandwave Dynamics, 23–24.

Francken F, Wartel S, Parker R, Taveniers E, 2004. Factors influencing subaqueous dunes in the Scheldt Estuary. *Geo-Marine Letters* 24: 14–21. https://doi.org/10.1007/s00367-003-0154-x

Fryberger S, Dean G, 1979. Dune forms wind regime Chap F in A Study of Global Sand Seas, E.D. McKee ed. U.S. Geological Survey Professional Paper 1052, Chapter: F.

Greeley R, Iversen JD, 1985. Wind as a geological process: On Earth, Mars, Venus and Titan. Cambridge University Press. https://doi.org/10.1017/CBO9780511573071

Hersen P, 2004. On the crescentic shape of barchan dunes. *European Physical Journal B* 37: 507–514. https://doi.org/10.1140/epjb/e2004-00087-y

Hersen P, Douady S, Andreotti B, 2002. Relevant length scale of barchan dunes. *Physical Review Letters* 89(26): 264301. https://doi.org/10.1103/PhysRevLett.89.264301

Howard AD, Morton JB, Gad-el-Hak M, Pierce DB, 1978. Sand transport model of barchan dune equilibrium. *Sedimentology* 25(3): 307–338. https://doi.org/10.1111/j.1365-3091.1978.tb00316.x

Hugenholtz CH, Wolfe SA, 2005. Biogeomorphic model of dunefield activation and stabilization on the northern Great Plains. *Geomorphology* 70(1–2): 53–70. https://doi.org/10.1016/j.geomorph.2005.03.011

Lancaster N, 1995. Geomorphology of desert dunes. Routledge, London.

Ma X, Yan J, Hou Y, Lin F, Zheng X, 2016. Footprints of obliquely incident internal solitary waves and internal

tides near the shelf break in the northern South China Sea. *Journal of Geophysical Research: Oceans* 121. https://doi.org/10.1002/2016JC012009

Melo HPM, Parteli EJR, Andrade JS Jr., Herrmann HJ, 2012. Linear stability analysis of transverse dunes. *Physica A: Statistical Mechanics and its Applications* 391(20): 4606–4614. https://doi.org/10.1016/j.physa.2012.05.042

Prandle D, 1985. On salinity regimes and the vertical structure of residual flows in narrow tidal estuaries. *Estuarine, Coastal and Shelf Science* 20(5): 615–635. https://doi.org/10.1016/0272-7714(85)90111-8

Rubanenko L, Lapôtre MGA, Ewing RC, Fenton LK, Gunn A, 2022. A distinct ripple-formation regime on Mars revealed by the morphometrics of barchan dunes. *Nature Communications* 13: 7156. https://doi.org/10.1038/s41467-022-34974-3

Sauermann G, Kroy K, Herrmann HJ, 2001. Continuum saltation model for sand dunes. *Physical Review E* 64(3): 031305. https://doi.org/10.1103/PhysRevE.64.031305

Schwämmle V, Herrmann HJ, 2005. A model of Barchan dunes including lateral shear stress. *European Physical Journal E* 16: 57–65. https://doi.org/10.1140/epje/e2005-00007-0

Sun H, Li YF, Xie BT, 2024. Formation, evolution, and influencing factors of nearshore sand waves and sand ridges in the southwestern coastal area of Hainan Island. *Advances in Marine Science*. https://doi.org/10.12362/j.issn.1671-6647.20240301002

Terwindt JHJ, 1971. Sand waves in the southern bight of the North Sea. *Marine Geology* 10(1): 51–67. https://doi.org/10.1016/0025-3227(71)90076-4

Van Dijk PM, Arens SM, van Boxel JH, 1999. Aeolian processes across transverse dunes. II: Modelling the sediment transport and profile development. *Earth Surface Processes and Landforms* 24(4): 319–333.

Van Dijk PM, Kleinhans MG, 2005. Predicting bedform response to flow variability. *Earth Surface Processes and Landforms* 30(6): 687–703.

Van Landeghem KJJ, Wheeler AJ, Mitchell NC, Sutton G, 2009. Variations in sediment wave dimensions across the tidally dominated Irish Sea, NW Europe. *Marine Geology* 263: 108–119.

Van Rijn LC, 1984. Sediment transport, part II: suspended load transport. *Journal of Hydraulic Engineering* 110(11): 1613–1641.

Van Rijn LC, 2007. Unified view of sediment transport by currents and waves. II: Suspended transport. *Journal of Hydraulic Engineering* 133(6): 668–689.

Van Rijn LC, Kroon A, 1993. Sediment transport by currents and waves. *In Proceedings of the 23rd International Conference on Coastal Engineering*, 2613–2628. ASCE.

Xia D, Wu R, Liu Z, Yin P, Bian F, Ye Y, Xie Q, Chen X, Lai X, Chen X, 2001. Study on the activity of submarine sand waves off the eastern coast of Hainan Island. *Journal of Oceanography of Huanghai & Bohai Seas* 19(1): 1–8. (in Chinese)

Xie B, Sun H, Liu T, Tan H, 2024. Investigation of the local scour depth of a pile foundation on the migrating sand waves seabed in the western South China Sea. *Frontiers in Earth Science* 12: 1404430. https://doi.org/10.3389/feart.2024.1404430

Yalin MS, 1972. Mechanics of sediment transport. Pergamon Press, Oxford.

Zhang Y, Lin Y, He N, Gao X, Yang B, 2024. Local similarity between aeolian barchan dunes and their downsized subaqueous counterparts. *Journal of Geophysical Research: Earth Surface* 129(5): e2023JF007617. https://doi.org/10.1029/2023JF007617

Zhou J, Wu Z, Jin X, Zhao D, Cao Z, Guan W, 2018. Observations and analysis of giant sand wave fields on the Taiwan Banks, northern South China Sea. *Marine Geology* 406: 132–141. https://doi.org/10.1016/j.margeo.2018.09.015

中文概要

题　目： 海南岛西部近岸水下新月形沙丘的形态动力学及控制机制

作　者： 孙杭[1,2,3]，张琪[2]，谢波涛[2]，苗波[4,5]，王立忠[1]，李国鑫[6]，李昱霏[7]，高秦[8]

机　构： [1]浙江大学海洋学院，中国舟山，316021；[2]中海油研究总院工程研究设计院，中国北京，100028；[3]全省海洋土木工程与材料浙江省重点实验室，中国杭州，310058；[4]亥姆霍兹海岸系统分析与建模研究所，德国盖斯特哈赫特，21502；[5]汉堡大学海洋学研究所地球系统研究与可持续发展中心，德国汉堡，20148；[6]中海油天津分公司，中国天津，300450；[7]中海油田服务股份有限公司，中国天津，300459；[8]东南大学南通海洋高等研究院，中国南通，226010

目　的： 本文旨在基于海南岛西部近海两期多波束水深地形实测数据，系统刻画水下新月形沙丘的几何形态特征及其动态演化过程，揭示潮流动力、泥沙输运、悬浮泥沙浓度和水深条件对沙丘形成、迁移和形态稳定性的控制机制。研究进一步探讨水下沙丘是否存在形态发育上限及其主控因素，以期为复杂海域海底地貌演化、区域泥沙动力过程分析以及海洋工程安全评价提供理论依据和工程参考。

创新点： 1. 基于两期高分辨率多波束实测地形数据，系统揭示了海南岛西部近海水下新月形沙丘的形态

参数、迁移特征和动态演化规律；2. 阐明了潮流动力、推移质输运、悬浮泥沙滞后效应和水深限制共同控制沙丘形成与发育的机制. 。

方　法： 1. 通过观测数据，采用快速傅里叶变换方法提取典型地形剖面的相位差，计算沙丘在主导水动力方向上的迁移距离和迁移速率，结合潮流动力、泥沙输运和水深条件，建立沙丘形态演化与环境控制因素之间的关系；2. 通过计算摩阻流速与泥沙沉降速度之比，判别研究区泥沙输运方式；利用单位宽度输沙率和涨落潮净输沙通量，分析潮流作用下泥沙输运强度与方向性；进一步引入虚拟边界层理论，探讨水深、流速和粒径对沙丘临界高度及形态稳定性的控制作用。

结　论： 1. 沙丘的形成与演化受水动力条件、泥沙输运特征和水深等多因素共同控制；2. 沙丘高度在决定水下新月形沙丘形态稳定性和水动力响应方面起主导作用，沙丘宽度与高度和波长均表现出明显的线性相关关系，因而是连接垂向生长与水平发育过程的关键形态参数；3. 新月形沙丘的生长过程包括起始、追赶、合并和分裂四个阶段，其形态演化依次表现为新月形、弯曲形、分叉形和线性沙丘。水深通过调节潮流条件，对沙丘临界高度具有重要控制作用。同时，泥沙供给显著影响沙丘波长和形态，是驱动沙丘系统动态演化的关键因素。

关键词： 水下沙丘；潮流动力；悬浮泥沙；生长尺度；水深控制；动态演化